Stony Brook University

Identification of specific residues necessary for the eviction of H2A.Z-containing nucleosomes

A Thesis Presented

by

Karole Nicole D'Orazio

to

The Graduate School

in Partial Fulfillment of the

Requirements

for the Degree of

Master of Science

in

Biochemistry and Cellular Biology

Stony Brook University

December 2013

Stony Brook University

The Graduate School

Karole Nicole D'Orazio

We, the thesis committee for the above candidate for the

Master of Science degree, hereby recommend

acceptance of this thesis.

Dr. Ed Luk
Assistant Professor in the Department of Biochemistry and Cell Biology

Dr. Nancy M. Hollingsworth
Professor in the Department of Biochemistry and Cell Biology

This thesis is accepted by the Graduate School

Charles Taber
Dean of the Graduate School

Abstract of the Thesis

Identification of specific residues necessary for the eviction of H2A.Z-containing nucleosomes

by

Karole D'Orazio

Master of Science

in

Biochemistry and Cellular Biology

Stony Brook University

2013

In this study, I investigated how the well-conserved histone variant H2A.Z is removed from promoters to prepare genes for transcription. H2A.Z is found at the majority of nucleosomes near promoters in place of the canonical histone H2A. Why H2A.Z is localized to gene promoters in all eukaryotes is unclear. One hypothesis is that H2A.Z marks nucleosomes for disassembly, thereby opening up promoters to give room for the transcription machinery to assemble. How H2A.Z-containing nucleosomes are removed from promoter sites is also unknown, but the Luk laboratory has recently found that ATP is necessary for this process. We propose that there may be an evictor enzyme that specifically recognizes H2A.Z and removes it from promoters. Although H2A and H2A.Z can assemble together with H2B, H3, H4 and DNA into nucleosomes that are structurally similar, 40% of the amino acids in the polypeptides of H2A and H2A.Z differ. This thesis tests the hypothesis that the putative evictor may recognize some of the unique residues of H2A.Z to mediate nucleosome disassembly. The genes *HTZ1* and

HTA1 encode H2A.Z and H2A in yeast, respectively. Using a collection of yeast expression vectors bearing various domain swap genes of *HTZ1* and *HTA1*, the unique amino acid residues of Htz1 that are important for histone eviction were looked for. Substitution of Htz1 sequences required for eviction with the corresponding region of Hta1 should result in a loss of function and failure to complement the phenotype of *htz1*Δ yeast. Nine domain swap (Htz1/Hta1) proteins that failed to fully complement the *htz1*Δ phenotype in yeast were identified. The Htz1/Hta1 protein-containing strains that failed to complement were then assayed for their enrichment at promoters by chromatin immunoprecipitation (ChIP) and qPCR assays. Our model predicts that proteins defective for recognition by the evictor protein will accumulate at promoters. However, none of these chimeric proteins accumulate at promoters. Instead, all of these Htz1/Hta1 proteins are depleted at promoters relative to wild-type Htz1 and five of them have lost some or all of their ability to accumulate at promoters. The data suggest that these proteins lack the Htz1-specific residues important for promoter specific deposition. Furthermore, the data support the idea that the specific residues important in promoter specific deposition of Htz1 are located in the α1 helix, loop1 and α2 helix regions of Htz1.

Table of Contents

List of Figures

List of Abbreviations

H2A	Histone two A
Hta1	Histone two A one
H2A.Z	Histone two A Z
Htz1	Histone two Z one
H3	Histone three
H4	Histone four
α	Alpha
S. cerevisiae	*Saccharomyces cerevisiae*
ChIP	Chromatin immunoprecipitation
IP	Immunoprecipitation
Nu+1	Nucleosome +1
Nu+2	Nucleosome +2
ORF	Open reading frame
CSM –URA	Complete synthetic media lacking uracil
FM	Formamide
Bp	Base pairs
Nt	Nucleotides
WT	Wild-type
qPCR	Quantitative polymerase chain reaction
3D	Three dimensional
ATP	Adenosine triphosphate
NFR	Nucleosome free region

PDB	Protein database
SGD	*Saccharomyces* genome database
K	Lysine
Ac	Acetylation
SDS	Sodium dodecyl sulfate
TSS	Transcription start site
OD	Optical density
TE	Tris EDTA
EDTA	Ethylenediaminetetraacetic Acid
PBS	Phosphate-buffered saline
DNA	Deoxyribonucleic acid
Rpm	Rotations per minute

Acknowledgements

I would like to thank Dr. Ed Luk for accepting me into his lab and for the time he has dedicated to advising and mentoring me on all of my goals. With his help, I have learned valuable scientific techniques and great problem solving skills. His encouragement and guidance has led to my success with graduate school applications and I know I would not be where I am today without his help.

I would like to acknowledge the rest of the Luk lab as well for all of their assistance along the way. A special thanks to Lihong Wan, Michael Tramantano, Lu Sun, Christina Roman, and Won Kyun Koh for their support.

I would also like to thank Dr. Nancy Hollingsworth for her advice and assistance on my projects and future goals. She has served as a great role model for me and is a great role model for any aspiring scientist.

I. Introduction:

1. Structure of chromatin:

The human genome is made up of ~3 billion base pairs of highly negatively charged DNA which must be organized to allow precise control of transcription and DNA replication. The nucleosome is the most fundamental packing unit of chromatin organization. It consists of a protein core that is made up of positively charged histone proteins and 147 base pairs of DNA (Luger et al., 1997). The nucleosomal DNA coils in left handed, superhelical turns around the histone octamer made up of two dimers of H2A-H2B and two dimers of H3-H4 (Figure 1A) (Luger et al., 1997). Each histone dimer comes together through a histone fold domain (Luger et al., 1997). When the nucleosome forms, stabilization of the DNA comes from 14 sites of contact between the histone octamer and the minor grooves of the DNA (Bowman, 2010). Inside the cell, nucleosomes are separated by linker DNA, a fragment of DNA that averages ~18 base pairs in *Saccharomyces cerevisiae* and greater in higher eukaryotes (Barski et al., 2007; Mavrich et al., 2008). The string of nucleosomes connected by linker DNA makes up chromatin.

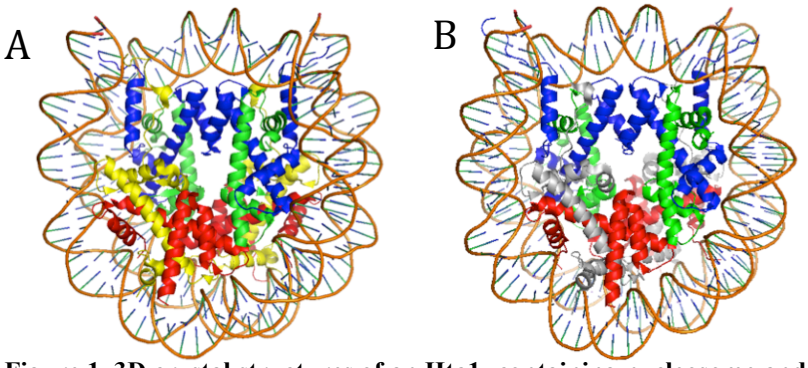

Figure 1. 3D crystal structures of an Hta1- containing nucleosome and an HTZ1-containing nucleosome.
A) 3D crystal structure of the *S. cerevisiae* nucleosome containing 146 base pairs of DNA with 3.1Å resolution. Hta1 is in yellow; H2B is in red; H3 is in blue; H4 is in green. Modified from RCSB PDB 1ID3 structure identified by White et. Al. (White et al., 2001).
B) 3D crystal structure of the Htz1-containing nucleosome, with the Htz1 protein crystalized from Homo sapiens. 146 bp of DNA are shown and the structure is resolved to 2.6Å. Htz1 is in white; H2B is in red; H3 is in blue; H4 is in green. Modified from RCSB PDB 1F66 structure identified by Suto et. Al. (Suto et al., 2000).

Chromatin structure varies within an organism. An extended linker DNA, called an nucleosome free region (NFR), is frequently found upstream of

transcription start sites in *S. cerevisiae* (Lee et al., 2007). The nucleosome closest to the transcription start site is referred to as the +1 nucleosome and for most promoters it presents an obstacle for the assembly of transcriptional machinery (Jiang and Pugh, 2009). Therefore, the +1 nucleosome must be partially or fully removed at some point during transcription to allow for transcriptional initiation.

2. Histone Variant H2A.Z

In budding yeast, the majority of +1 nucleosomes of both active and inactive genes contain a histone variant of H2A, H2A.Z (Guillemette et al., 2005). While the canonical histones, H2A, H2B, H3 and H4, are deposited in chromatin during S-phase of the cell cycle, histone variants, including H2A.Z, H3.3 and H2A.X, are deposited in all stages of the cell cycle and play various biological functions (Kamakaka and Biggins, 2005). Although H2A.Z is found at sites other than the +1 nucleosome, its positioning at the +1 nucleosome site will be the focus of this paper because this is essential in controlling gene expression (Santisteban et al., 2000; Wan et al., 2009). H2A.Z's function is unclear, but it is hypothesized to poise the downstream gene for transcription by creating a nucleosome that is more prone to disassembly than the canonical H2A-containing nucleosome.

H2A.Z is well conserved throughout eukaryotes (Talbert and Henikoff, 2010). Additionally, the gene for H2A.Z is essential in metazoans and a deletion of the H2A.Z gene in yeast (*HTZ1)* causes defects in growth, transcription, and DNA repair (Santisteban et al., 2000; Wan et al., 2009). The primary structure of Htz1 is 60% identical to the canonical H2A protein, which is encoded for by the yeast genes, *HTA1* and *HTA2* (Figure 2A). The Hta1 and Hta2 proteins differ by two amino acids in the C-terminus, but appear to be functionally equivalent (Kolodrubetz et al., 1982). The secondary structure of Htz1 and Hta1 (or Hta2) are very similar

in that each has a helix fold domain consisting of an α1 helix, α2 helix, and α3 helix and a C-terminal helix domain called the αC helix (Figure 1B, 2B and 2C). The α1 and α2 helices are connected by a loop of amino acids that are referred to as loop1 and the α2 and α3 helices are connected by a loop of amino acids that are referred to as loop2. Figure 2D highlights residues

A

```
Hta1   1    MSG-GKGGKAGSAAK-----ASQSRSAKAGLTFPVGRVHRLLRRGNYAQ-RIGSGAPVYL  53
            MSG   GGK  S AK      SQS SA+AGL FPVGR+ R L+R    + R+GS A +YL
Htz1   1    MSGKAHGGKGKSGAKDSGSLRSQSSSARAGLQFPVGRIKRYLKRHATGRTRVGSKAAIYL  60

Hta1   54   TAVLEYLAAEILELAGNAARDNKKTRIIPRHLQLAIRNDDELNKLLGNVTIAQGGVLPNI  113
            TAVLEYL AE+LELAGNAA+D K  RI PRHLQLAIR DDEL+ L+   TIA GGVLP+I
Htz1   61   TAVLEYLTAEVLELAGNAAKDLKVKRITPRHLQLAIRGDDELDSLI-RATIASGGVLPHI  119

Hta1   114  HQNLLPKKSAKATK  127
            ++ LL K   K +K
Htz1   120  NKALLLKVEKKGSK  133
```

B

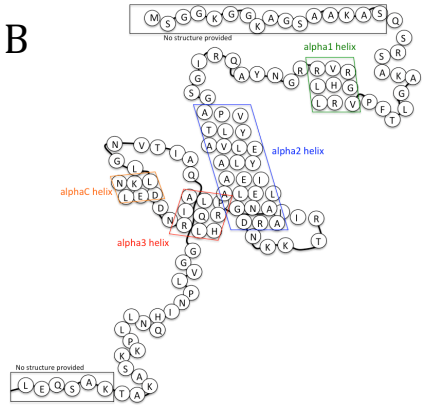

C

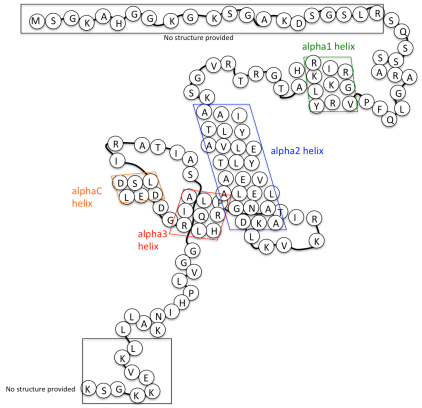

D

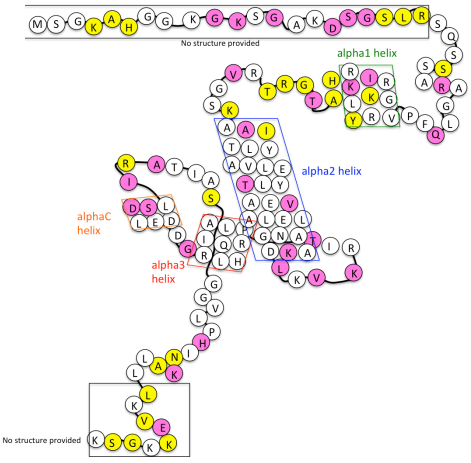

Figure 2. The primary and secondary structures of Hta1 and Htz1
A) Primary structures of Hta1 and Htz1 proteins with 60% identity shown. The top line is the sequence of Hta1, the bottom line is the sequence of Htz1, and the middle line is the residues that are alike between the two proteins or similar. '+' symbol represents a residue that is similar. Sequences obtained from SGD and alignment performed using BLAST.
B) Secondary structure of the *S. cerevisiae* Hta1 protein (Modified from RCSB PDB 1ID3 structure of Hta1 identified by White et al. (White et al., 2001) and using the amino acid sequence obtained by SGD)
C) Secondary structure of the *S. cerevisiae* Htz1protein (Modified from RCSB PDB structure of the human H2A.Z 1F66 identified by Suto et al. (Suto et al., 2000) and using the amino acid sequence of the yeast Htz1 obtained from SGD).
D) Secondary structure of the *S. cerevisiae* Htz1 protein. Residues highlighted in yellow differ between Hta1 and Htz1. Residues highlighted in purple differ between Hta1 and Htz1 in yeast and are conserved (identical) throughout yeast, flies and humans (Modified from RCSB PDB structure identified by White et al. (White et al., 2001)).

that are found in Htz1, not found in Hta1 and conserved throughout yeast, flies, and humans (Figure 2D, pink). These residues are likely essential to Htz1's specific function due to their conservation throughout eukaryotes and their absence in Hta1.

These unique amino acid residues of Htz1 may serve as a binding surface for other proteins. For example, the histone chaperone Chz1, a protein that may be an early player for the incorporation of Htz1 onto chromatin, binds with higher affinity to Htz1-H2B dimers than to Hta1-H2B dimers (Luk et al., 2007). However, if the αC helix of Hta1 is replaced with the αC helix of Htz1, then Chz1 preferentially binds to the mutated Hta1[αC] protein over the wild-type Hta1 protein (Luk et al., 2007). Therefore, the unique residues of the C-terminal α helix of Htz1 play a role in the Chz1-Htz1 interaction. Through this relatively strong interaction, Chz1 may then place the Htz1-H2B dimer in close vicinity of the machinery that puts Htz1-H2B into chromatin.

3. The Deposition Mechanism of H2A.Z

The placement of Htz1-H2B dimers into promoter site nucleosomes also involves the unique residues that are found and conserved in Htz1, but not Hta1. Htz1-H2B dimers are exchanged for Hta1-H2B dimers at promoters, a reaction catalyzed by a 14-subunit chromatin remodeling complex called SWR1 (Mizuguchi et al., 2004). In vitro, this complex specifically recognizes the amino acid region from 98 to 108 of Htz1, called the M6 region, as shown by another domain swap experiment in which the M6 region of Hta1 (amino acids 91 to 102) was replaced with the M6 region of Htz1. This resulted in SWR1 obtaining an affinity towards the Hta1[M6]-H2B dimer similar to SWR1's affinity for the Htz1-H2B dimer (Wu et al., 2005). Therefore, specific residues in the M6 domain of Htz1 interact with a binding domain of SWR1. After SWR1 binds the Htz1-H2B dimer, it is targeted to the promoter by its strong affinity for

the long stretches of naked DNA found at the NFR region (Nguyen et al., 2013) and promoter-specific histone modifications, such as H3K14Ac and H3K9Ac (Raisner et al., 2005). SWR1 then catalyzes the histone replacement reaction, exchanging the nucleosomal Hta1-H2B dimers with free Htz1-H2B dimers in an ATP-dependent manner (Figure 3A) (Mizuguchi et al., 2004). The ATPase activity of SWR1 required for this exchange is hyper-stimulated only when it is simultaneously bound to an Hta1 containing nucleosome and an Htz1 containing dimer (Luk et al., 2010; Mizuguchi et al., 2004). This supports SWR1 having an affinity for Hta1-containing nucleosomes over Htz1-containing nucleosomes, perhaps due to the unique residues of Hta1.

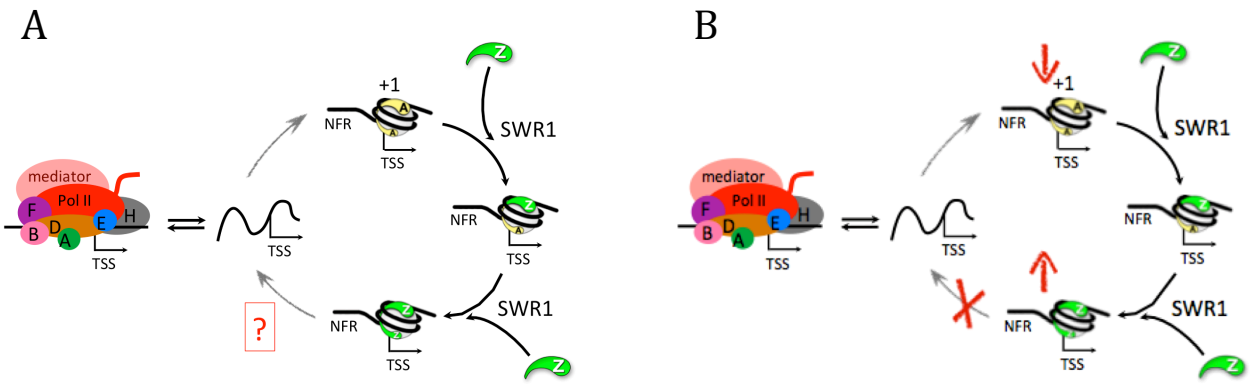

Figure 3. Proposed cycle of Htz1 and Hta1 deposition and eviction
A) Proposed cycle of Htz1 and Hta1 deposition and eviction with possible evictor enzyme. "Z" represents an Htz1-H2b dimer and "A" represents an Hta1-H2B dimer.
B) Expected result of mutation in domain that evictor protein recognizes. If the domain of Htz1 recognized by the evictor protein is mutated, you expect to see an accumulation of Htz1 at promoter sites.

4. The Proposed Cycle of Htz1 at Promoters

Knowing the deposition mechanism of Htz1-H2B dimers, we hypothesize that there is a cycle at promoter sites where Htz1-H2B dimers replace Hta1-H2B dimers, the nucleosome disassembles, and Hta1-H2B-containing nucleosomes are reassembled (Figure 3A). This cyclical pathway is supported by data that shows Hta1-H2B-containing nucleosomes, Htz1-H2B-containing nucleosomes and Hta1-H2B/ Htz1-H2B heterotypic nucleosomes can all be found at the same promoter (Luk et al., 2010) and that the SWR1 reaction is unidirectional (Luk et al.,

2010). Additionally, the presence of the intermediate heterotypic nucleosome suggests that the exchange process of SWR1 likely occurs one dimer at a time. However, there must be a pathway converting the Htz1-containing state to the Hta1-containing state. We hypothesize the pathway from the Htz1 state to the Hta1 state involves an intermediate configuration in which there is naked DNA at the transcription start site (TSS) due to disassembly of the Htz1-containing nucleosome. Supporting this idea is the evidence of H3 having a higher turnover rate at promoters than at open reading frame regions (Dion et al., 2007). Since H3 is at the core of the nucleosome, H3 turnover implies that the nucleosome must be fully disassembled, as opposed to partially disassembled (Figure 3A). Furthermore, nucleosome disassembly and reassembly is hypothesized to involve an Hta1-containing nucleosome replacing an Htz1-containing nucleosome.

5. Exploring The Eviction Mechanism of Htz1

The proposed cycle requires a process of eviction of Htz1-containing nucleosomes at promoter sites, which is currently unknown. It has been shown that Htz1-containing nucleosomes are more unstable in high salt (Jin and Felsenfeld, 2007; Zhang et al., 2005), suggesting an intrinsic instability of Htz1 nucleosomes could explain nucleosome disassembly at promoters. However, such in vitro salt sensitivity experiments may not reflect in vivo stability of Htz1 nucleosomes. In fact, the salt required to disrupt Htz1 nucleosomes in some experiments is non-physiologically high (Watanabe et al., 2013; Zhang et al., 2005). Unpublished data from our group have shown that when cells are treated with sodium azide, blocking ATP production (i.e. all active processes inside the cell), Htz1 levels remain the same for over 2 hours (Michael Tramantano unpublished data). Therefore, we propose that there must be an active pathway in which an evictor enzyme is required for the disassembly of Htz1-containing nucleosomes.

We hypothesize that since the putative evictor protein is preferentially disassembling nucleosomes containing Htz1 over those containing Hta1, the evictor is likely recognizing unique residues of Htz1 not found in Hta1. If this is true, mutations that replace the Htz1-specific residues with the Hta1-specfic residues are expected to prevent the evictor from recognizing and disassembling the mutant Htz1-containing nucleosomes, resulting in an accumulation of mutant Htz1-containing nucleosomes at promoter regions (Figure 3B).

In the following experiments, regions of *HTZ1* were mutated to the corresponding regions of *HTA1*, the gene encoding for Hta1, and transformed into *htz1*Δ *S. cerevisiae*. Then, using spotting assays, the ability of the domain swap proteins to rescue yeast strains lacking the endogenous Htz1 was tested. However, hybrid proteins that failed to rescue *HTZ1* deficient strains could potentially be defective for deposition onto chromatin, eviction from chromatin, or other unknown functions. Therefore, to distinguish the domain swap proteins with a defect in eviction from the others, chromatin immunoprecipitation (ChIP) analysis was used. ChIP determined if any of the domain swap proteins accumulated at promoters relative to wild-type Htz1. Surprisingly, none of the mutants accumulated at the promoters. Instead, I did observe that some proteins were unexpectedly depleted at promoter sites. This suggests these proteins may be defective for deposition and therefore the regions mutated may be important for recognition by SWR1 deposition machinery.

II. Materials and Methods

1. Plasmids/Hybrid Proteins

All vectors used in the experiments were originated from the yeast shuttle plasmid, pRS416, containing either the *HTZ1* or *HTA1* gene under the control of the endogenous *HTZ1* promoter. The histone genes are fused in-frame with the 2xFLAG epitope tag at the C-terminus. The *htz1/hta1* hybrid mutants were previously generated by standard site-directed mutagenesis and cloning procedures using the episomal *HTZ1* and *HTA1* plasmids as templates (Wu et al., 2005, unpublished reagents of Ed Luk and Jon Backus). The sequence integrity of the coding region of the *htz1/hta1* genes was verified by DNA sequencing (*Stony Brook University, DNA sequencing facility*).

Figure 4. Schematic of hybrid protein structure resulting from the expression of plasmids containing mutated *htz1*. 2 FLAG tags on each protein are not displayed. Red represents Htz1 regions; yellow represents Hta1 regions.

2. Spotting Assay

Wild-type and *htz1*Δ mutant yeast strains were transformed with the various plasmids using the standard lithium acetate procedure (Gietz and Schiestl, 1991). Transformants were selected on complete synthetic dextrose medium lacking uracil (CSM –URA). The growth rate of the transformants was analyzed by spotting assays. Briefly, transformed cells were resuspended in sterile H_2O at an optical density of one at 600 nm (OD_{600} = 1) and serially diluted 10 fold. The suspensions were then spotted onto CSM –

URA plates with or without 2% formamide. The plates were incubated at 30˚C for 2 days before imaged by the FLA4010 CCD camera (*GE Healthcare*).

3. ChIP

Transformants carrying the wild-type *HTZ1* and *HTA1* plasmids as well as *htz1/hta1* mutant plasmids were analyzed with chromatin immunoprecipitation using a procedure modified from Komarnitsky et al., 2000.

To start, 250 ml cultures of the various transformed strains of yeast were grown to OD_{600} ~0.5 in CSM –URA supplemented with 10 ml of 2 mg/ml adenylyl sulfate. The cells were fixed with 1% formaldehyde for 20 minutes. 25 ml of 3 M glycine was added to stop crosslinking. Cells were then pelleted and washed 2 x in 200 ml 1 x TBS (20 mM Tris-HCl, pH 7.5, and 150 mM NaCl). They were then resuspended in 10 ml FA lysis buffer/0.1% SDS (50mM Hepes-KOH, 150 mM NaCl, 1 mM EDTA, 1% Triton X-100, 0.1% Na Deoxycholate and 0.1% SDS). Cells were pelleted again.

For lysis, cells were resuspended in 800 µl FA lysis buffer/0.5% SDS and beaten with zirconia beads in a Biospec Products mini-beadbeater. The lysed cell solution was diluted with 6.5 ml FA lysis buffer/0.1% SDS and centrifuged at 45,000 rpm for 20 min in a Beckman 50 Ti type rotor within a Beckman L8-80M ultracentrifuge. The supernatant was discarded. The pellet was then resuspended in 6.5 ml FA lysis buffer/0.1% SDS and centrifuged at 45,000 rpm for 20 min again. The supernatant was discarded and the pellet was resuspended in 1.5 ml FA lysis buffer/0.1% SDS for sonication.

A microtip was used to sonicate the chromatin to ~200-300 bp fragments with the sample tube submerged in an ice water bath. Sonication was performed at 40% power for 5 min, with 10 sec rests between each 10 sec pulse. The sonicated solution was diluted with 6.5 ml FA lysis

buffer/0.1% SDS and centrifuged at 45,000 rpm for 20 min a third time. The supernatant was stored at -80ºC. Aliquots were used for immunoprecipitation (IP).

To prepare bead-bound antibodies for IP, 100vμl of Dynabeads-coupled Protein G beads (Invitrogen) were incubated with 40 μg of affinity purified mouse monoclonal anti-FLAG M2 antibody (Sigma-Aldrich) or ~40 μg of anti-H2B rabbit antibody (Luk et al., 2007) in 200μl 1x PBS buffer for 2 hours at room temperature. These bead-bound antibodies were washed with 1ml of FA lysis buffer/0.1%SDS. Then 800 μl sonicated chromatin aliquots were thawed and 20 μl of 5 M NaCl was added such that the final concentration of NaCl was 27 5mM. 700 μl of the resulting chromatin solution was incubated with the bead-bound antibodies at 4ºC overnight. 50 μl of the remaining chromatin solution was saved as the INPUT control. After the overnight incubation, the IP reaction was pelleted, washed 2 x with buffer 1 (1 ml of FA lysis buffer/0.1% Triton X-100/275 mM NaCl), incubated in this buffer at RT for 4 minutes on a rotator, then pelleted and resuspended in buffer 2 (1 ml of FA lysis buffer/0.1% Triton X-100/500 mM NaCl). This was repeated for buffers 2, 3 (1 ml of 10 mM Tris-HCl, pH 8.0, 0.25 M LiCl, 1 mM EDTA, 0.5% NP-40) and 4 (1 ml of TE (10 mM Tris-HCl, pH 8.0, 1 mM EDTA)). After the washes, 250 μl of elution buffer containing 50 mM Tris-Hcl, pH 7.5, 10 mM EDTA, and 1% SDS along with 12.5 μl of Proteinase K were applied to the beads, which represent the IP sample. For the INPUT control, 200 μl of the elution buffer and 12.5 μl of Proteinase K were added. These IP and INPUT samples were left at 55ºC for 1 hr then 65ºC over night. The supernatant of the beads was transferred to a new tube and the beads were washed with 250 μl TE. 250 μl of TE was added to the INPUT samples. 50 μl 4 M LiCl was added to all samples. DNA was extracted by standard phenol/chloroform extraction, followed by a chloroform

extraction, followed by an ethanol precipitation. The samples were resuspended in 100 µl TE and qPCR was used for analysis.

4. Gel Analysis of Sonication Product

To control for fragmentation size of the chromatin, the chromatin before and after sonication was analyzed by agarose electrophoresis. 25 µl aliquots of the unsonicated and sonicated samples were set aside. 4 µl of Proteinase K and 200 µl of SGEN buffer (1% SDS, 0.25 µg/µl glycogen, 20 mM EDTA, and 0.2 M NaCl) were added to the aliquots. These samples were then incubated for 1 hr at 55ºC then shifted to 65ºC over night. Phenol/chloroform extraction and ethanol precipitation were performed to extract the DNA. The DNA was pelleted, resuspended in 45 µl of TE along with 5 µl RNase (Roche), and left overnight at 37ºC. 10 µl of the sample was analyzed on a 1.3% agarose/0.5 x TBE gel at 100 V for 30 min in 0.5 x TBE. The gel was stained with 1 x SYBR Green in 0.5 x TBE for 2 hr and then imaged using the FLA4010 imager.

5. Western Blot Analysis

To control for efficiency of the anti-FLAG and anti-H2B IP reactions, samples of the INPUT and the "flow-through" (FT) fraction (supernatant after the IP) were analyzed by western blotting. The samples were mixed with Laemmli buffer at a final concentration of 1 x and were heated at 95ºC for 30 min before analyzed on a 14% polyacrylamide Tris-Glycine gel at 150 V for 1 hr 25 min in 1x TGS buffer. The proteins were then transfered to a 0.22 µm PVDF membrane (Bio-Rad) at 25 V for 2 hrs in 1x transfer buffer (20% methanol, 1x TG (7.2 g Glycine and 1.5 g Trizma Base), and 0.1% SDS) using the Novex apparatus (Invitrogen). The membrane was blocked with 2% GE Advance blocking agent in 1 x TTBS (1 x TBS, and 0.1% Tween 20) plus 0.05% NaN_3 and then blotted with a guinea pig anti-Htz1 antibody (at 1:1000

dilution) or rabbit anti-H2B antibody (at 1:5000) for 1 hr or overnight at 4ºC. Membranes were washed with 1 x TTBS solution three times before blotted with the corresponding secondary antibodies conjugated with horseradish peroxidase (HRP). The resulting membranes were washed with 1 x TTBS before developed with the ECL reagents (ECL Prime, GE Healthcare).

6. qPCR

Quantitative PCR analysis of the INPUT and IP samples was performed using the Roche Lightcycler 480 on 384-well plates. Each qPCR reaction contained 2.5 µl of 4µM primer mix, 2.5 µl diluted DNA, and 5 µl 2 x Roche FastStart master mix. The qPCR program used is as follows:

		1x
1	95 ˚C	5 min
2	95 ˚C	10 sec
3	60 ˚C (ramp 2.5˚C/sec)	20 sec
4	72 ˚C	10 sec
5	Read plate	
6	Repeat steps (2-5) 39x more times	
7	Melting curve 50-95 ˚C, read every 0.3 ˚C	
8	95˚C	3 min
9	Decrease to 72 ˚C with ramp rate @ 0.1 ˚C/sec	
10	72 ˚C	1 min
11	22 ˚C	1 min

The primers used are listed here and named by the gene and the region of the gene they amplify, respectively. SSK2 Nu+1: GTTGCTGTGTATTCAGTATATCC; SOL2/SSK2 Nu+1: GAATTGAGGATGCTAAGCTAATG; SNT1 ORF: ATTCGTCAACAAGAAAAATTGG; SNT1 ORF: TACTTTCCGGAGTTGAACTAGTG; Pat1 Nu+1: TAACTCTCTTCAAAGTCCAGAGGA; Pat1 Nu+1: TAAGAGCAGCAAGAAGCACTAGCA; Pat1 Nu+2: TGCAACATATGATCTAGCCGTG; Pat1 Nu+2: TTTTGGAAATCCTCACAGCAGC; RIM15 ORF: CTAGTTCATCACCGGCACCAAC;

RIM15 ORF: CTTGTTTGTGAGCCTATACCGATTC. The regions of these genes have been shown to be H2A.Z rich or H2A.Z depleted and this information is listed in Figure 7A.

III. Results

1. Complementation test to screen for potential Htz1 eviction mutants

The eviction function of Htz1 is critical for its transcriptional function and therefore any mutations that are defective for eviction should exhibit a loss of function phenotype and fail to rescue the slow growth phenotype of *HTZ1* deficient yeast. To identify loss of function mutants, an *htz1*Δ mutant strain was transformed with plasmids bearing the *htz1*/*hta1* genes and the growth rates were compared to look for complementation using a spotting assay. To enhance the contrast of growth defects in *htz1*Δ cells relative to wild-type cells, I supplemented the growth medium with + 2% formamide (FM).

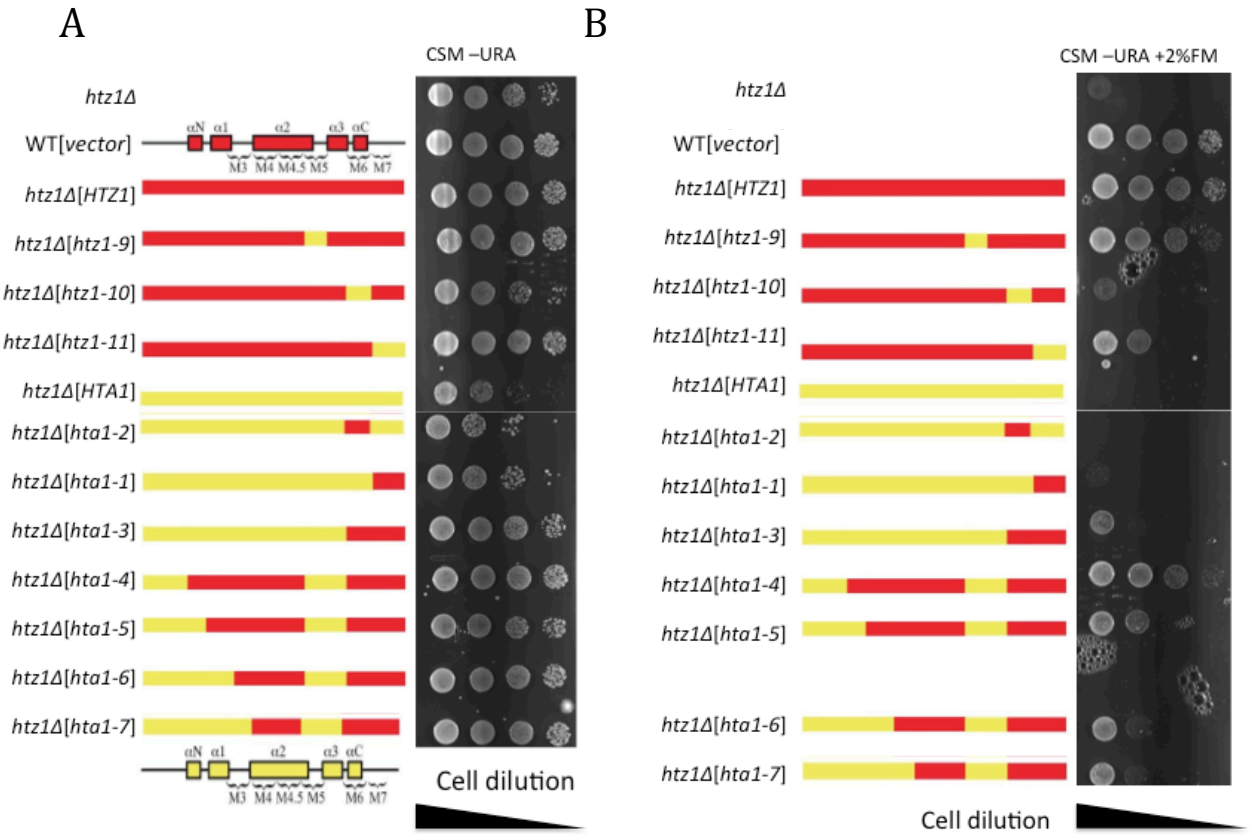

Figure 5. Spotting assay of different strains of *S. cerevisiae* transformed with various domain swap plasmids. Listed to the left in both A and B are the strain of yeast with the plasmid that was inserted listed in brackets. 2 FLAG tags are not shown, but are encoded for immediately downstream of each domain swap gene.
A) *htz1*Δ *S. cerevisiae* transformed with plasmids to the right and grown on CSM-URA plate.
B) *htz1*Δ *S. cerevisiae* transformed with plasmids to the right and grown on CSM-URA/2% formamide plate.

Consistent with published results, *htz1*Δ cells transformed with an empty vector failed to grow on 2% FM plates (Figure 5, right panel, row 1). By contrast, *htz1*Δ cells transformed with the wild-type *HTZ1* gene (Figure 5, right panel, row 3) restored the growth rate as in wild-type cells carrying the empty vector (Figure 5, right panel, row 2). Since the *HTZ1* gene, as well as the *htz1*/*hta1* chimeric genes, are epitope tagged with 2xFLAG and the endogenous *HTZ1* is untagged, the similar growth rate between *htz1*Δ[*HTZ1-2xFLAG*] and WT[empty vector] suggests that the 2xFLAG tags did not interfere with Htz1 function.

Analysis of the assay led to the conclusion that most of the domain swap proteins cannot fully restore the slow growth phenotype of *htz1*Δ cells on 2% FM media. *HTA1, htz1-10, hta1-1,* and *hta1-2* genes failed to rescue *htz1*Δ cells. *htz1-11, hta1-3, hta1-5, hta1-6* and *hta1-7* genes gave a weak rescue effect, while *htz1-9* and *hta1-4* gave a modest rescue effect. Since eviction mutants are expected to lose Htz1 function, *hta1-1, hta1-2, hta1-1, hta1-5, hta-6, hta1-7, htz1-10,* and *htz1-11* may represent potential eviction mutants. Mutants *htz1-1* through *htz1-8* (Figure 4) were not tested because they were previously shown to fully rescue the *htz1*Δ phenotype (Ed Luk unpublished data); therefore, they were unlikely to be defective for eviction.

2. Using ChIP to identify eviction mutants that accumulate at promoters

Domain swap proteins that failed to rescue *htz1*Δ cells may be defective for eviction but may also be defective for promoter-specific deposition. Therefore, to distinguish whether the proteins are defective for deposition or eviction, I performed ChIP analysis to measure the level of chromatin-bound chimeric proteins.

Sonication was performed to fragment and solubilize the chromatin before the IP step. Since the size of the fragmented chromatin limits the resolution of the ChIP analysis, I analyzed the size of the chromatin DNA by agarose gel electrophoresis before and after the sonication

step. Figure 6A shows that after 5 min of sonication, the majority of the DNA was fragmented to 200-400 bp. This suggests that chromatin sites centered > 1000 bp apart should not be significantly influenced by the neighboring ChIP signal.

IP of the domain swap proteins was performed using an anti-FLAG antibody since the proteins (as well as the wild-type Htz1 and Hta1 controls) are fused in-frame with a 2x-FLAG epitope tag. To control for IP efficiency, the INPUT and flow-through (FT) samples were analyzed by western blotting. Figure 6B shows ~50% of Htz1-2FLAG was immunodepleted by the anti-FLAG pull-down (Figure 6B). By contrast, less than 10% of H2B is immunodepleted by the anti-H2B antibody. This suggests that more antibodies or less INPUT material should be used for this IP reaction.

The genomic locations and the sequences of the primer pairs used in the qPCR analysis are summarized in Figure 7A. Based on previous microarray data (Luk et al., 2010), three Htz1-enriched sites (A, C, and D) at +1 and +2 nucleosomal positions were chosen along with two Htz1-depleted sites (B and E) in open reading frame (ORF) regions (Figure 7B).

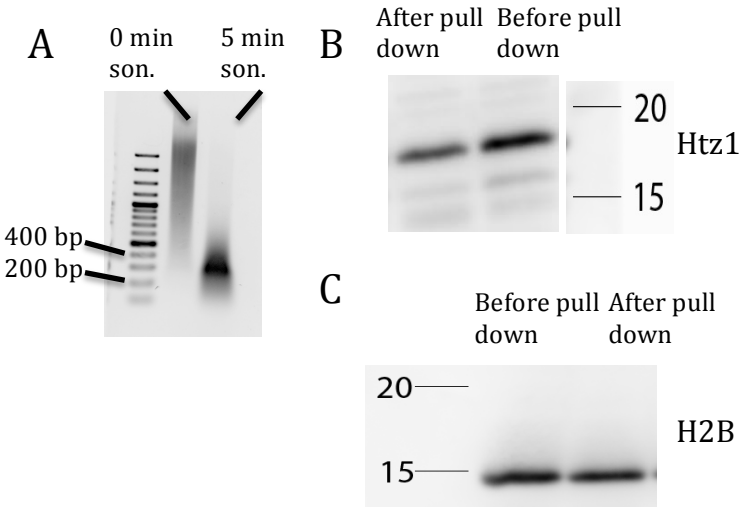

Figure 6. Sonication and immunoprecipitation efficiencies.
A) Gel analysis of ChIP DNA before sonication (t=0) and after sonication (t=5 min). "son." = sonicated.
B) Western blot analysis of IP efficiency. Htz1 detection using HTZ1 antibody. IP efficiency ~50%.
C) Western blot analysis of IP efficiency. H2B detection using H2B antibody.

A

Genomic Region	*SSK22* +1 Nucleosome	*SNT1* ORF	*PAT1* +1 Nucleosome	*PAT1* +2 Nucleosome	*RIM15* ORF
Genomic Region Abbreviation	A	B	C	D	E
Location	Chr3 246549-246650	Chr3 186779-186863	Chr3 252557-252649	Chr3 252382-252467	Chr6 69414-69514

B

Region A

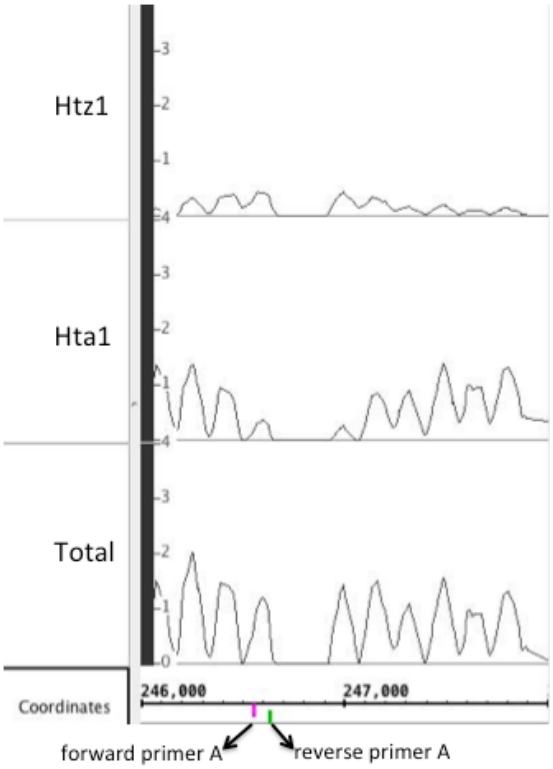

Region B

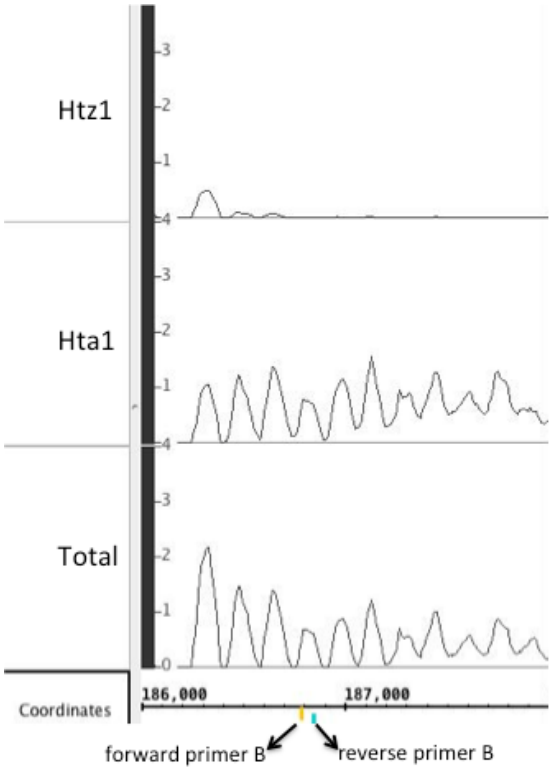

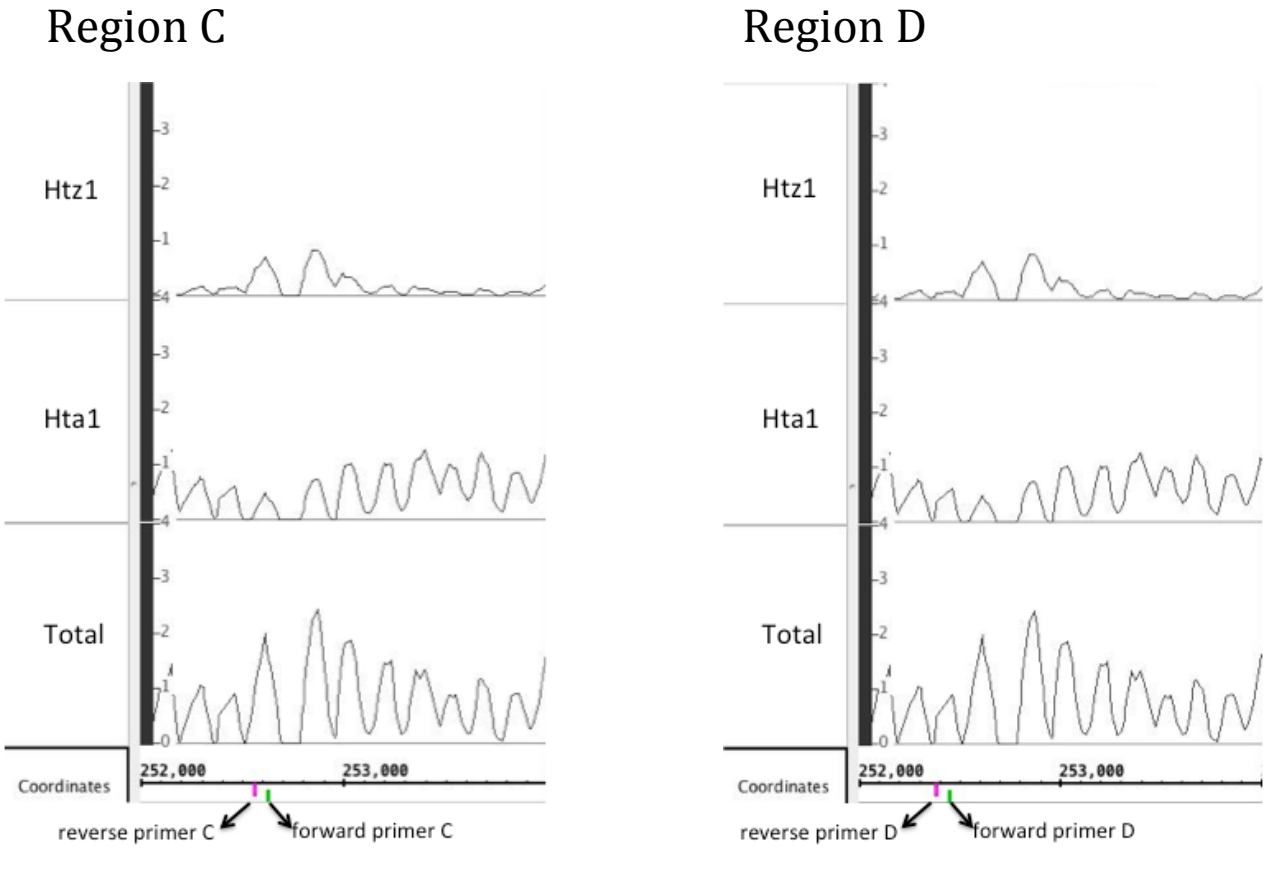

Figure 7. Specifics regarding regions amplified by the designated primers used for qPCR.
A) List of the genomic regions the primers amplified. In parentheses are the systematic names of the genes. The abbreviations used throughout the paper are listed below the genomic region which they represent.
B) Microarray data analyzed using IGB from previous work done in the lab by Ed Luk. The left labels indicate if the signal represents an "Htz1" signal, "Hta1" signal, or a "TOTAL" signal, which is all nucleosomes. The Figure is spanning ~2000 nt, specifically around the site that the designated primers amplify.

The qPCR data for the anti-FLAG ChIP experiment are presented as % INPUT for regions A-E. Consistent with published results, Htz1-2xFlag is enriched at the promoters relative to the ORF regions. The combined ChIP signals at A, C, and D as compared to the combined signals at B and E gives ~5:1 preference for promoter deposition over ORF deposition for the Htz1-2xFlag protein (Figure 8, row 1: column 1). By contrast, Hta1-2xFlag gave a ~1:2 ratio of deposition at the promoters compared to ORFs, showing a preference for ORF deposition over promoter deposition (Figure 8, row 1: column 2). Htz1-10, Htz1-11, Htz1-4, and Htz1-5 containing mutants all showed a preference for promoter over ORF similar to Htz1 containing mutants (Figure 8, row 1: column 3, row 2: column 1, row 3: column 2, row 3: column 3, respectively), while Hta1-1, Hta1-2, and Hta1-3 showed a ratio of promoter to ORF similar to Hta1 (Figure 8, row 2: column 2, row 2: column 3, row 3: column 1, respectively). *htz1*Δ cells containing Htz1-6 and Htz1-7 showed a ratio of promoter to ORF deposition that fell in between these two groups (Figure 8, row 4: column 1, row 4: column 2, respectively).

It was somewhat surprising that Htz1-10 showed promoter enrichment at a level comparable to Htz1. Htz1-10, which has the M6 region of Htz1 replaced with the corresponding region from Hta1, is expected to be defective for promoter-specific deposition because the M6 region of Htz1 is the portion recognized by the deposition machinery SWR1. This led us to question whether the ratio of ChIP signals at promoters versus ORF sites is an accurate measurement of Flag-tagged protein incorporation. In addition, the % INPUT values for Htz1 enriched sites (e.g. primer pair A) are significantly lower for Htz1-10 compared to wild-type Htz1. Therefore, the steady-state occupancy of the Flag-tagged Htz1-10 may be lower. However, an alternative explanation for the variation of % INPUT for a specific site among the samples

could be that the IP efficiency varies among the ChIP experiments. To control for IP efficiency, I performed H2B ChIP and normalized the Flag ChIP signal to that of H2B.

Figure 9 shows that all domain swap proteins and Hta1 exhibited a decreased presence at promoters as compared to the Htz1 promoter presence, after correction for H2B occupancy (Figure 9). Although the normalized occupancies of Hta1 and Hta1-7 proteins are the highest of all proteins tested, their deposition efficiencies were still three-fold lower than Htz1. Since spotting assays showed some domain swap proteins like Htz1-4 gave close to wild-type levels of complementation, the reason that these deposition efficiencies are lower than Htz1's is contradictory to previous results. We currently don't have an explanation for the data but will speculate in the next section.

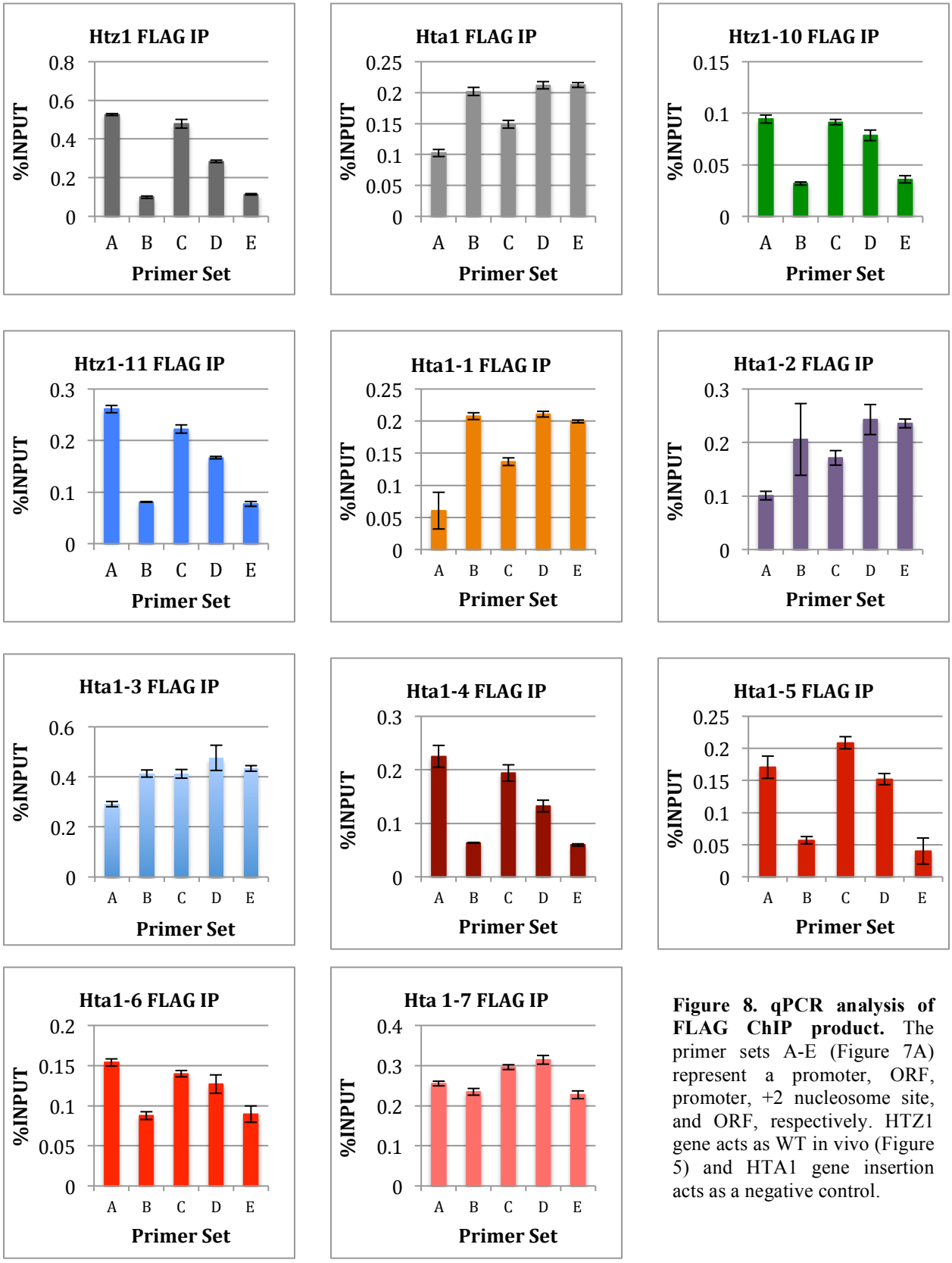

Figure 8. qPCR analysis of FLAG ChIP product. The primer sets A-E (Figure 7A) represent a promoter, ORF, promoter, +2 nucleosome site, and ORF, respectively. HTZ1 gene acts as WT in vivo (Figure 5) and HTA1 gene insertion acts as a negative control.

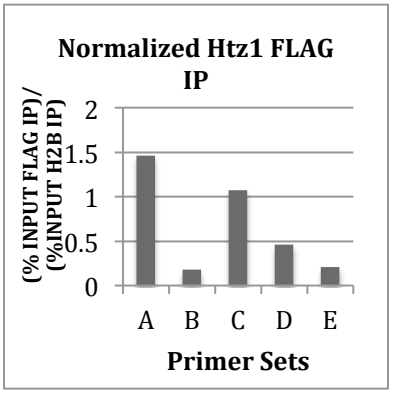

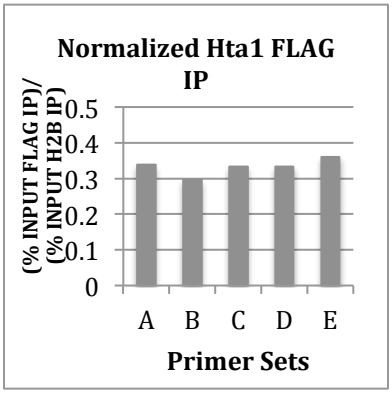

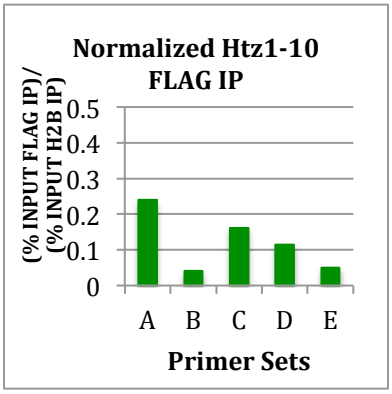

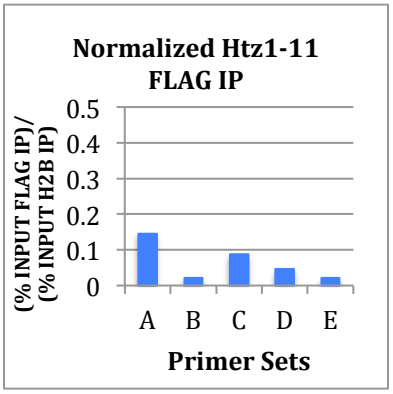

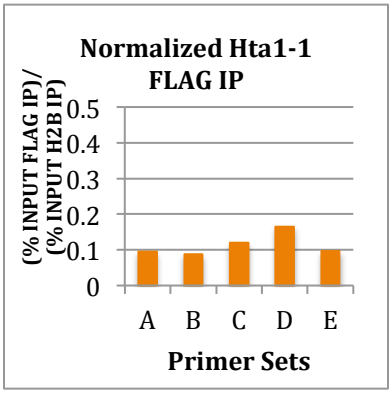

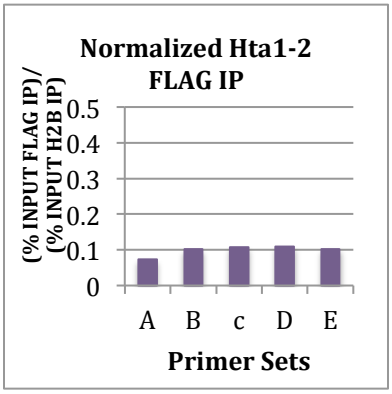

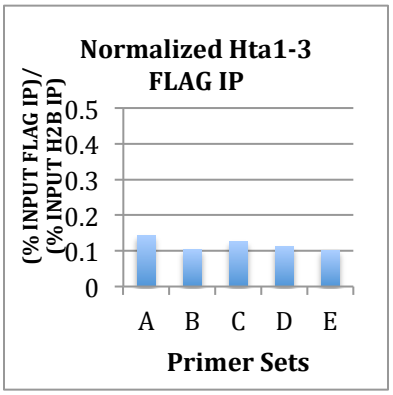

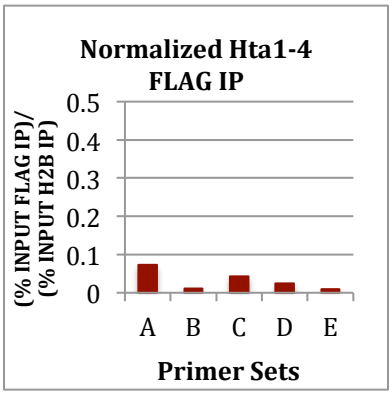

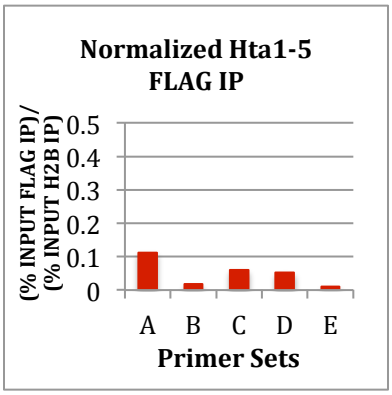

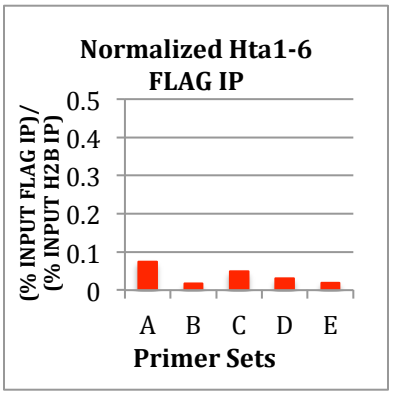

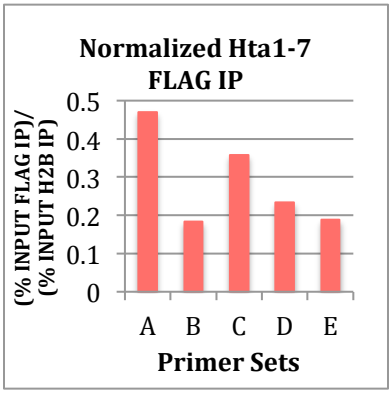

Figure 9. qPCR analysis of FLAG ChIP product / H2B ChIP Product. Normalization of % INPUT of FLAG IP obtained by dividing values in Fig 8 by %I NPUT of H2B IP. The primer sets (Figure 7a) A-E represent a promoter, ORF, promoter, +2 nucleosome site, and ORF, respectively. HTZ1 gene acts as WT in vivo (Figure 5) and HTA1 gene insertion acts as a negative control. Deposition efficiency = (% INPUT FLAG IP)/(% INPUT H2B IP)

IV. Discussion:

My ChIP data in Figures 8 and 9 show that none of the mutants tested exhibited accumulation at promoter sites. This suggests that the mutants are unlikely to be defective for eviction, but are possibly defective for deposition. A possible explanation for a lack of an eviction mutant is that the site(s) essential for eviction is identical to the site(s) that is essential for deposition. Therefore, when this site is mutated, the protein is not deposited at normal levels so it will not have the chance to accumulate at promoter sites. Additionally, the multiple deposition mutants identified give way to the idea that multiple sites on H2A.Z are essential for deposition.

When comparing the FLAG IP ChIP data of hta1-5 and hta1-3, we observed a dramatic "switch" from an Htz1-like pattern (i.e. high ChIP signals at A, C, and D relative to B and E) to an Hta1-like pattern (i.e. high ChIP signals at B, D, and E relative to A and C) (Figure 8, row 3: column 3, row 3: column 1, respectively). The amino acid residues responsible for the switch are localized in the α1 helix, loop1, and the α2 helix regions and highlighted in Figure 10. These three regions will be combined to be called the "switch" region hereafter. The switch region encompasses residues that are mutated when hta1-5 is mutated to hta1-3. We conclude that more than one residue in the switch region is important for the switch due to the intermediate phenotypes seen in hta1-6 and hta1-7. Additionally, we hypothesize the regions essential for the switch are those that are conserved throughout eukaryotes. These residues important in the promoter-specific deposition of HTZ1 are highlighted in Figure 11A. Figure 11B depicts the 3D structure of metazoan H2A.Z with these residues highlighted as well. How the switch region plays a role in promoter specific deposition is still unclear. SWR1, the deposition machinery recognizes H2A.Z at the M6 region, however, the M6 region is not sufficient for deposition.

Thus, the switch region may be important for the process of SWR1 loading Htz1 onto chromatin due to the interactions between this region and nucleosomal DNA. Supportive of this idea is Figure 11B showing that the highlighted switch residues are in close proximity to the DNA of the nucleosome. Additionally, Hta1 interacts with nucleosomal DNA via its α1 helix and loop1 region (Bowman, 2010). Thus, similar to Hta1, the switch region of Htz1 could provide an interaction surface with DNA, allowing the deposition machinery to effectively place Htz1-H2B dimers at promoter sites. However, why the Hta1-specfic residues would hinder this deposition process remains unclear.

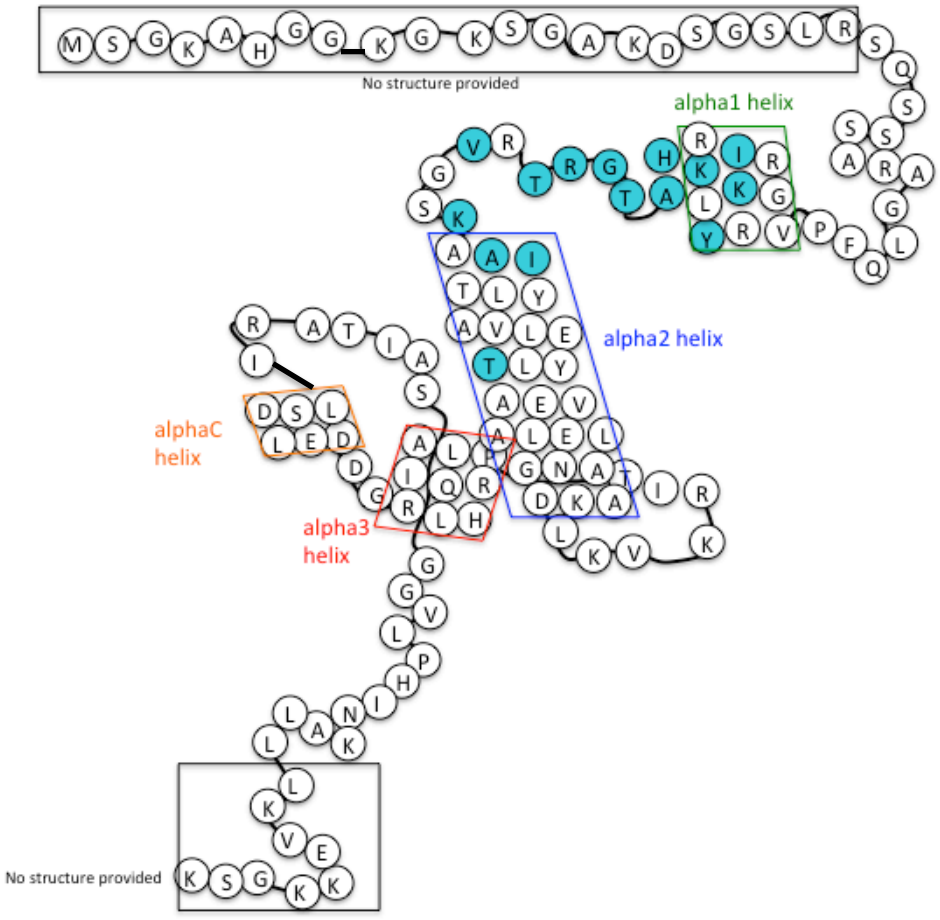

Figure 10. Highlighted residues that differ between H2A.Z and H2A, specifically within the switch region. Shown is the secondary structure of the *S. cerevisiae* H2A.Z protein. Residues highlighted in blue are residues essential for the switch from an H2A.Z acting protein to an H2A acting protein, in which the protein is no longer preferentially deposited at the promoter sites (modified from RCSB PDB structure identified by White et al. (White et al., 2001)).

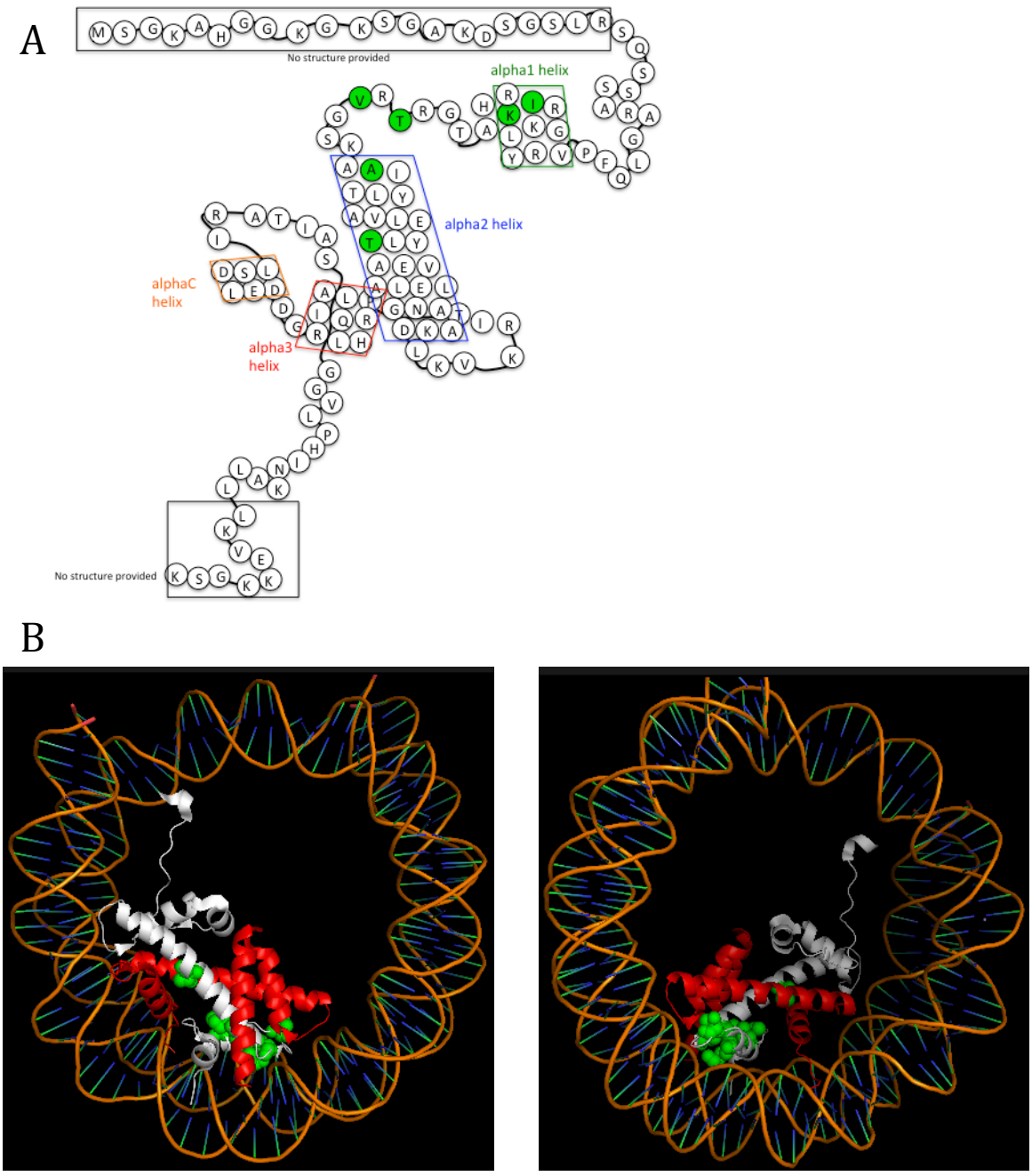

Figure 11. Highlighted residues that differ between H2A.Z and H2A and are conserved, specifically within the switch region.

A) Secondary structure of the *S. cerevisiae* H2A.Z protein. Residues highlighted in green are residues essential for the switch from an H2A.Z acting protein to an H2A acting protein, and conserved throughout yeast, flies and humans (modified from RCSB PDB structure identified by White et al. (White et al., 2001)).

B) 3D crystal structure of the H2A.Z containing nucleosome, with only one set of the H2A.Z and H2B histones. The H2A.Z protein was crystalized from Homo sapiens. 146 bp of DNA are shown and the structure is resolved to 2.6Å. The white cartoon represents H2A.Z, the red cartoon represents H2B and the residues highlighted in green in the form of a space fill model are those essential for the switch from an H2A.Z acting protein to an H2A acting protein, and conserved throughout yeast, flies and humans. Modified from RCSB PDB 1F66 structure identified by Suto et. Al. (Suto et al., 2000).

Approachable problems with IP efficiency throughout this project could be resolved with further experimentation. For example, the spotting assay that shows *hta1-4* almost fully rescues the *htz1*Δ strain suggests that this domain swap mutant is likely deposited normally onto the chromatin and able to normally perform Htz1 specific functions (e.g. deposition and eviction). However, the normalized ChIP data contradicts this interpretation as hta1-4 is only incorporated at ~5-10 % of the Htz1 level at promoter sites (Figure 9, row 1: column 1, row 3: column 2, respectively, regions A, C, and D). This led us to question whether the normalized ChIP data accurately reflects the absolute levels of the chromatin-bound domain swap mutants. Although anti-FLAG western analysis showed that the FLAG-tagged hybrids are expressed at levels similar to the wild-type Htz1 (Ed Luk unpublished data), this result does not inform on whether the histones are actually incorporated into chromatin. A more robust approach is to isolate the chromatin first before quantification of the domain swap-histone content by quantitative western. This approach bypasses the need of an IP, thereby eliminating any potential artifact due to IP efficiency. Finally, another approach to address the potential fluctuation of IP efficiency is to repeat the ChIP procedure for the same samples multiple times and to see how much variance is observed. As such, any conclusions and trends would be determined with statistical confidence.

In parallel with my thesis project, our lab has been searching for protein factors that actively remove Htz1. Recently, work of our colleagues showed that the transcriptional pre-initiation complex might play an active role in Htz1 eviction (Michael Tramantano unpublished data). In the future, we could perform a protein-protein interaction study between the domain swap mutants and components of the preinitation complex to look for eviction mutants. This would avoid the problem of domain-swap mutant incorporation into chromatin because we would look for an interaction between the eviction machinery and the domain-swap mutants.

References

Barski, A., Cuddapah, S., Cui, K., Roh, T.-Y., Schones, D.E., Wang, Z., Wei, G., Chepelev, I., and Zhao, K. (2007). High-resolution profiling of histone methylations in the human genome. Cell *129*, 823–837.

Bowman, G.D. (2010). Mechanisms of ATP-dependent nucleosome sliding. Curr. Opin. Struct. Biol. *20*, 73–81.

Dion, M.F., Kaplan, T., Kim, M., Buratowski, S., Friedman, N., and Rando, O.J. (2007). Dynamics of replication-independent histone turnover in budding yeast. Science *315*, 1405–1408.

Gietz, R.D., and Schiestl, R.H. (1991). Applications of high efficiency lithium acetate transformation of intact yeast cells using single-stranded nucleic acids as carrier. Yeast Chichester Engl. *7*, 253–263.

Guillemette, B., Bataille, A.R., Gévry, N., Adam, M., Blanchette, M., Robert, F., and Gaudreau, L. (2005). Variant histone H2A.Z is globally localized to the promoters of inactive yeast genes and regulates nucleosome positioning. PLoS Biol. *3*, e384.

Jiang, C., and Pugh, B.F. (2009). Nucleosome positioning and gene regulation: advances through genomics. Nat. Rev. Genet. *10*, 161–172.

Jin, C., and Felsenfeld, G. (2007). Nucleosome stability mediated by histone variants H3.3 and H2A.Z. Genes Dev. *21*, 1519–1529.

Kamakaka, R.T., and Biggins, S. (2005). Histone variants: deviants? Genes Dev. *19*, 295–310.

Kolodrubetz, D., Rykowski, M.C., and Grunstein, M. (1982). Histone H2A subtypes associate interchangeably in vivo with histone H2B subtypes. Proc. Natl. Acad. Sci. U. S. A. *79*, 7814–7818.

Komarnitsky, P., Cho, E.J., and Buratowski, S. (2000). Different phosphorylated forms of RNA polymerase II and associated mRNA processing factors during transcription. Genes Dev. *14*, 2452–2460.

Lee, W., Tillo, D., Bray, N., Morse, R.H., Davis, R.W., Hughes, T.R., and Nislow, C. (2007). A high-resolution atlas of nucleosome occupancy in yeast. Nat. Genet. *39*, 1235–1244.

Luger, K., Mäder, A.W., Richmond, R.K., Sargent, D.F., and Richmond, T.J. (1997). Crystal structure of the nucleosome core particle at 2.8 A resolution. Nature *389*, 251–260.

Luk, E., Vu, N.-D., Patteson, K., Mizuguchi, G., Wu, W.-H., Ranjan, A., Backus, J., Sen, S., Lewis, M., Bai, Y., et al. (2007). Chz1, a nuclear chaperone for histone H2AZ. Mol. Cell *25*, 357–368.

Luk, E., Ranjan, A., Fitzgerald, P.C., Mizuguchi, G., Huang, Y., Wei, D., and Wu, C. (2010). Stepwise histone replacement by SWR1 requires dual activation with histone H2A.Z and canonical nucleosome. Cell *143*, 725–736.

Mavrich, T.N., Ioshikhes, I.P., Venters, B.J., Jiang, C., Tomsho, L.P., Qi, J., Schuster, S.C., Albert, I., and Pugh, B.F. (2008). A barrier nucleosome model for statistical positioning of nucleosomes throughout the yeast genome. Genome Res. *18*, 1073–1083.

Mizuguchi, G., Shen, X., Landry, J., Wu, W.-H., Sen, S., and Wu, C. (2004). ATP-driven exchange of histone H2AZ variant catalyzed by SWR1 chromatin remodeling complex. Science *303*, 343–348.

Nguyen, V.Q., Ranjan, A., Stengel, F., Wei, D., Aebersold, R., Wu, C., and Leschziner, A.E. (2013). Molecular architecture of the ATP-dependent chromatin-remodeling complex SWR1. Cell *154*, 1220–1231.

Raisner, R.M., Hartley, P.D., Meneghini, M.D., Bao, M.Z., Liu, C.L., Schreiber, S.L., Rando, O.J., and Madhani, H.D. (2005). Histone variant H2A.Z marks the 5' ends of both active and inactive genes in euchromatin. Cell *123*, 233–248.

Santisteban, M.S., Kalashnikova, T., and Smith, M.M. (2000). Histone H2A.Z regulats transcription and is partially redundant with nucleosome remodeling complexes. Cell *103*, 411–422.

Talbert, P.B., and Henikoff, S. (2010). Histone variants--ancient wrap artists of the epigenome. Nat. Rev. Mol. Cell Biol. *11*, 264–275.

Wan, Y., Saleem, R.A., Ratushny, A.V., Roda, O., Smith, J.J., Lin, C.-H., Chiang, J.-H., and Aitchison, J.D. (2009). Role of the histone variant H2A.Z/Htz1p in TBP recruitment, chromatin dynamics, and regulated expression of oleate-responsive genes. Mol. Cell. Biol. *29*, 2346–2358.

Watanabe, S., Radman-Livaja, M., Rando, O.J., and Peterson, C.L. (2013). A histone acetylation switch regulates H2A.Z deposition by the SWR-C remodeling enzyme. Science *340*, 195–199.

Wu, W.-H., Alami, S., Luk, E., Wu, C.-H., Sen, S., Mizuguchi, G., Wei, D., and Wu, C. (2005). Swc2 is a widely conserved H2AZ-binding module essential for ATP-dependent histone exchange. Nat. Struct. Mol. Biol. *12*, 1064–1071.

Zhang, H., Roberts, D.N., and Cairns, B.R. (2005). Genome-wide dynamics of Htz1, a histone H2A variant that poises repressed/basal promoters for activation through histone loss. Cell *123*, 219–231.